Strength, Fracture and Complexity 3 (2005) 175–188
IOS Press

Scale effects on strength and toughness of grained materials: An extreme value theory approach

Alberto Carpinteri *, Pietro Cornetti and Simone Puzzi
Department of Structural Engineering and Geotechnics, Politecnico di Torino, Corso Duca degli Abruzzi 24, 10129 Torino, Italy

Abstract. The present paper provides a statistical model to the size effect on grained materials tensile strength and fracture energy. It has been already demonstrated by using extreme value theory that the scaling law obtained for the tensile strength introducing a doubly truncated distribution of flaws, under the hypothesis of Weibull's weakest link, resembles the Multi-Fractal Scaling Law (MFSL), already proposed by the first Author through fractal concepts. Since the weakest link in grained materials is usually represented by the interface between the matrix and the grains, in the present paper we assume that the flaw distribution can be represented by the grain size distribution, rather than by an arbitrary flaw distribution. Furthermore, introducing a micromechanical model for the critical displacement w_c, we draw a link between the fracture energy and the largest aggregate grain on crack surfaces. In this way we are able to compute the tensile strength and the fracture energy as a function of the specimen size. The obtained scaling laws are substantially in agreement with the MFSL for the fracture energy proposed by the first Author. A further result provided by the proposed approach is the description of the scatter increase of both tensile strength and fracture energy values when testing small specimens. This trend is confirmed by experimental data available in the literature. Eventually, the influence of the aggregate grading upon the size effect for strength and toughness is analyzed.

Keywords: Size effects, extreme value theory, grained materials

1. Introduction

With size effect we mean the dependence of one or more material parameters on the size of the material specimen. It is easy to realize the importance of this topic in engineering design. Recently, the scientific community dedicated significant efforts in order to have a consistent description of this phenomenon and to highlight the physical mechanisms that lie behind it. Dealing specifically with concrete structures, it was seen that tensile strength decreases with the structural size, whereas fracture energy increases [1,2]. In other words, the larger is the structure, the more brittle the structural behaviour results to be.

Aim of the present paper is to develop a statistical model providing the probability density function of grained materials tensile strength and fracture energy for specimens of different sizes. It has been already demonstrated by using extreme value theory [3] that the scaling law obtained for the tensile strength introducing a doubly truncated distribution of flaws, under the hypothesis of Weibull's weakest

*Corresponding author: Prof. Alberto Carpinteri, Chair of Structural Mechanics, Dept. of Structural Engineering and Geotechnics, Politecnico di Torino, Corso Duca degli Abruzzi, 24, 10129 Torino, Italy. Tel.: +39 011 564 4850; Fax: +39 011 564 4899; E-mail: alberto.carpinteri@polito.it.

link, resembles the Multi-Fractal Scaling Law (MFSL), already proposed by the first Author through fractal concepts [2]. The novelty of the present approach is that, since the interface between the matrix and the aggregates is the weakest link, we assume that the probability density function of the flaw sizes can be realistically represented by the probability density function of grain diameters [4]. Our analysis will therefore start with the description of the aggregate grading inside a grained material.

2. Microstructural analysis: The grain size distribution

The basis for the dimensional characterization of the aggregate is the sieve analysis. The sieve curve describes the weight fraction $W(d)$ of the aggregate passing through a sieve with d-wide mesh. Due to its good packing properties, the most common sieve curve used to prepare concrete is the so-called Füller curve:

$$W(d) = \sqrt{\frac{d}{\phi_{\max}}}. \tag{1}$$

Only in the last section we will deal with different distributions, pointing out the consequences upon size effects. Focusing the attention on the Füller distribution and assuming that the aggregates are spheres with diameter d comprised between $\phi_{\min}$ and $\phi_{\max}$, it can be easily shown [5] that the sieve curve represented by Eq. (1) can be expressed in terms of grain size distribution function as follows:

$$f_d(d) = \frac{2.5}{1-\alpha^{-2.5}} \frac{\phi_{\min}^{2.5}}{d^{3.5}}, \tag{2}$$

where $\alpha = \phi_{\max}/\phi_{\min}$ and $f_d(d)$ is a probability density function (PDF), i.e. $f_d(d)\,\mathrm{d}d$ is the fraction of grains with diameter belonging to the interval $[d, d+\mathrm{d}d]$ and the integral of $f_d(d)$ over the whole interval $[\phi_{\min}, \phi_{\max}]$ is equal to unity. Equation (2) shows clearly that the number of small particles is higher than that of the larger ones, since the former must fill the gaps between the latter ones. Note that the first denominator in the previous expression is very close to the unity; nevertheless, differently from other approaches [6], we cannot neglect it in the following computation since that term will be raised to very high exponents.

In order to link the concrete volume with the number of grains inside it, we need one more parameter, i.e., the volume percentage f_a of the aggregates. The total number of particles inside a volume V is therefore obtained, on average, dividing the total volume of aggregates inside the concrete volume by the average grain volume:

$$N = \frac{f_a V}{\pi/6\,\overline{d^3}}, \tag{3}$$

here $\overline{d^3}$ is the third moment of the PDF defined by Eq. (2):

$$\overline{d^3} = \int_{\phi_{\min}}^{\phi_{\max}} f_d(d) d^3\,\mathrm{d}d = \frac{5(1-\alpha^{-0.5})}{1-\alpha^{-2.5}} \phi_{\min}^{2.5} \phi_{\max}^{0.5}. \tag{4}$$

Following the procedure outlined by Carpinteri et al. [3], we compute the expression of the PDF of the maximum diameter of the N aggregate particles contained within a given volume V, defined as: $d_{\max} = \max\{d_1, d_2, \ldots, d_N\}$. We need the cumulative distribution function of the aggregate particle diameter, defined as the integral of the PDF (Eq. (2)):

$$F_d(d) = \int_{\phi_{\min}}^{d} f_d(x)\,\mathrm{d}x = \frac{1 - (\phi_{\min}/d)^{2.5}}{1 - \alpha^{-2.5}}. \tag{5}$$

Starting from the hypothesis that the N aggregate diameters are independent and identically distributed variables (this is not unnatural, because they come all from the same distribution), the extreme value theory provides the following equality chain, where P[event] represents the probability of that event to occur:

$$F_{d_{\max}}(d) = P[d_{\max} \leqslant d] = \prod_{i=1}^{N} P[d_i \leqslant d] = \prod_{i=1}^{N} F_{d_i}(d) = \big[F_d(d)\big]^N. \tag{6}$$

In the equality chain of Eq. (6), the second equality is justified by the independence and the last by the identical distribution assumption. By derivation it is now possible calculating the PDF of $d_{\max}$:

$$f_{d_{\max}}(d) = N\big[F_d(d)\big]^{N-1} f_d(d). \tag{7}$$

3. Size effect upon tensile strength

Now we derive the relation between the strength and the grain number. As stated in the introduction, we assume that the strength depends on the largest flaw according to Weibull's weakest link hypothesis. Furthermore, we assume that defect interactions are negligible and, due to interface weakness, we represent the effect of a spherical particle as that of a penny-shaped crack with the same diameter (Fig. 1). Hence we can write the ultimate tensile strength σ_u as:

$$\sigma_u(d_{\max}) = \frac{\pi}{\sqrt{2}} \frac{K_{IC}}{\sqrt{\pi d_{\max}}}, \tag{8}$$

where K_{IC} is the material toughness.

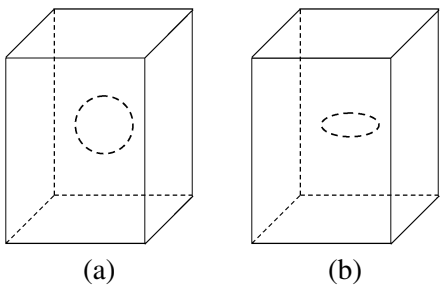

Fig. 1. The interfacial crack around grain boundary (a) is simply modelled by a penny shaped crack of the same diameter (b).

Equation (8) states that the tensile strength decreases along with the inverse of the square root of the largest grain diameter. The minimum strength is achieved when $d_{\max}$ is equal to $\phi_{\max}$ and is denoted by f_t. Thus Eq. (8) can be rewritten as:

$$\sigma_u(d_{\max}) = f_t \sqrt{\frac{\phi_{\max}}{d_{\max}}}. \tag{9}$$

From the previous equation, it is clear that σ_u is a statistical variable as long as $d_{\max}$. Therefore, the PDF of σ_u depends on the PDF of $d_{\max}$ according to the following relationship:

$$f_{\sigma_u}(\sigma_u) = f_{d_{\max}}(d) \left| \frac{\mathrm{d}\, d_{\max}}{\mathrm{d}\, \sigma_u} \right|. \tag{10}$$

The computation of the mean value of the tensile strength is now straightforward, since:

$$\overline{\sigma_u} = \int_{f_t}^{f_t\sqrt{\alpha}} \sigma_u f_{\sigma_u}(\sigma_u)\, \mathrm{d}\sigma_u. \tag{11}$$

Through the variable change provided by Eq. (9) and integrating by parts, the following expression for the average tensile strength can be derived as a function of the number N of grains:

$$\frac{\overline{\sigma_u}}{f_t} = 1 + \frac{\sqrt{\alpha}}{5(1-\beta)^N} B_{(\beta,1)}\left(\frac{1}{5}, N+1\right), \tag{12}$$

where $\beta = \alpha^{-2.5}$ and

$$B_{(a,b)}(n,m) = \int_a^b (1-x)^{m-1} x^{n-1}\, \mathrm{d}x \tag{13}$$

is the Generalized Incomplete Beta Function. The non-dimensional mean value of the tensile strength can be calculated by Eq. (12) as a function of the particles number N and of the parameter α. A first important remark is that only the ratio α between maximum and minimum aggregate size plays a role, whilst the value of the maximum diameter does not affect the function shape. The results are summarized in Fig. 2a, where the log–log plot evidences that all the curves exhibit a similar behaviour, with two distinct ranges. In the lowest one the curves decrease with a constant slope, approximately equal to 0.2, thus following a power law, whilst for larger values of N they present an asymptotic trend towards the unity. Physically speaking, this means that, increasing the number of particles considered, the probability of finding among them one with the maximum size approaches the unity, i.e. certainty. From a mechanical point of view, this yields an average tensile strength approaching f_t for sufficiently high N values.

To highlight the scale effect upon strength, we need the link between N and the structural size. Equation (3) provides the relationship between the number of grains N and the volume V. Observe that, in this case, (i) f_a is the volume fraction of grains showing an interfacial crack and (ii) V is the volume of the part of the specimen where the largest flaw must be sought, i.e. the higher stressed zone where final fracture may occur (it is not the bulk of the whole specimen). Introducing a length b proportional to the structural size of the specimen, we can distinguish two different cases:

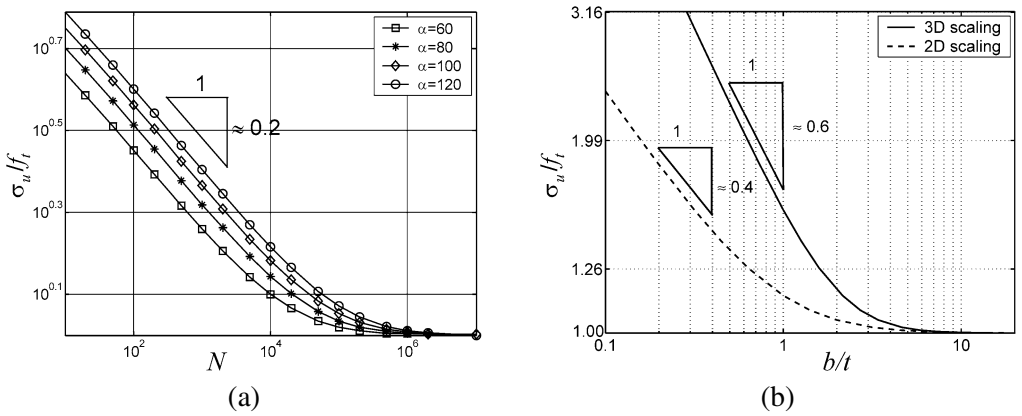

Fig. 2. Tensile strength as a function of the number of grains N surrounded by an interfacial crack (a) and size effect (b).

(a) Two-dimensional scaling: $V \approx b^2$,
(b) Three-dimensional scaling: $V \approx b^3$.

The consequent result is a set of different exponent values at small scales, whilst the behaviour at large scales is independent of the considered scaling type. The small-scale scaling are respectively the following:

(a) Two-dimensional scaling: $\sigma_u \approx b^{-0.4}$,
(b) Three-dimensional scaling: $\sigma_u \approx b^{-0.6}$.

These two types of asymptotic behaviour are summarized in the bi-logarithmic plot of Fig. 2b, where the structural size has been divided by a fixed length t (e.g. the specimen thickness for specimens with two-dimensional scaling). As can be easily argued, the higher is the order of scaling, the stronger is the size-scale effect.

4. Size effect upon fracture energy

In order to obtain the relationship between the fracture energy and the grain number, we start analyzing the effect of the largest grain diameter upon the critical displacement w_c, i.e. the distance at which interactions among crack lips vanish. The long tail usually shown by the cohesive laws of grained materials is due to the bridging action between the crack lips exerted by the grains (Fig. 3a). The larger are the grains, the larger is the distance between the lips at which the interaction vanishes. The final part of the softening regime is strictly related to the pull out of the largest grains. When a grain is pulled out from the matrix, interlocking between the grain and the matrix supplies the resistance to the separation of the plane. Of course, unlike fibre pull out, where the critical separation of the failure plane is on average equal to one fourth of the fiber length, the critical distance in grain pull out is much smaller than the aggregate radius, as shown by several experiments.

To carry on our analysis, we do not need the exact value of the critical distance: it is sufficient to know how it varies along with the grain diameter. Let us now remove for a while the hypothesis of spherical aggregates and consider the single grain (Fig. 3b). Denoting by η the difference between the maximum and minimum diameter of the grain (i.e. η is a roughness index), geometrical considerations allow us to conclude that, for a grain of diameter d, the distance at which the interaction between the crack surfaces

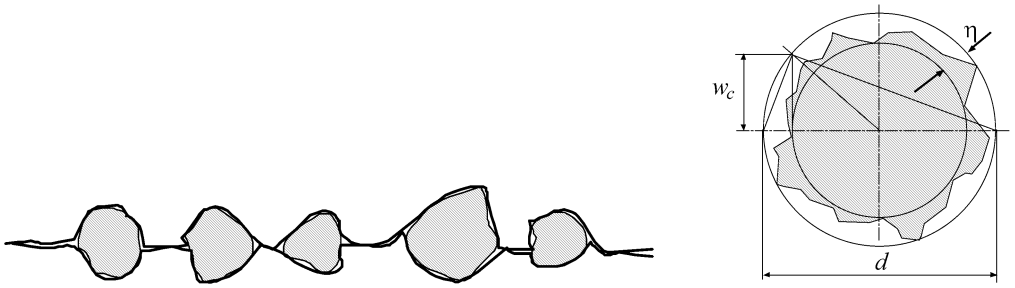

Fig. 3. Aggregates lying on the crack surface (a) and detail of a single grain (b) for the determination of the critical displacement w_c.

vanishes is given by $\sqrt{\eta d}$. Although different hypotheses can be formulated about the grain roughness, we will simply assume that $\eta \propto d$, i.e. the grains are self similar. The distance at which interaction vanishes is therefore proportional to d: it follows that the critical displacement is proportional to the diameter of the largest grain upon fracture surface, since it is the last one to be pulled out:

$$w_c = k_1 d_{\max}, \tag{14}$$

k_1 being a material constant. Note that, in analogy with Eq. (14), Eq. (8) for the tensile strength can be rewritten as $\sigma_u = k_2/\sqrt{d_{\max}}$. Again, k_2 is a material constant.

Assuming that the shape of the cohesive law is size independent, the dependence of the fracture energy with respect to $d_{\max}$ is straightforward. In fact, indicating by f the size independent function describing the dimensionless cohesive law yields:

$$\frac{\sigma}{\sigma_u} = f\left(\frac{w}{w_c}\right). \tag{15}$$

Equation (15) is equivalent to state that the dependence of the cohesive law on the structural size is only due to the size dependence of its peak (the tensile strength) and its tail (the critical displacement). Observe that this statement is also implicit in the fractal cohesive crack model presented by Carpinteri et al. [7]. According to its definition, we can compute the fracture energy from Eq. (15):

$$\mathcal{G}_{\mathcal{F}} = \int_0^{w_c} \sigma(w)\,\mathrm{d}w = w_c\sigma_u \int_0^1 f\left(\frac{w}{w_c}\right)\mathrm{d}\left(\frac{w}{w_c}\right) = w_c\sigma_u g_F = k_1 k_2 g_F \sqrt{d_{\max}}, \tag{16}$$

where g_F is the value of the integral: it is a dimensionless constant depending on the shape of the cohesive law (e.g. $1/2$ for a linear cohesive law). Equation (16) provides the dependence of the fracture energy upon the largest grain diameter $d_{\max}$ we were looking for. The same dependence of $\mathcal{G}_{\mathcal{F}}$ upon the largest grain diameter has been proposed on experimental evidence by several authors [8,9], so that the hypothesis stated in Eq. (14) is confirmed. Noting that in the limit of large specimen size $d_{\max}$ tends to $\phi_{\max}$, we can evaluate the ratio between fracture energy $\mathcal{G}_{\mathcal{F}}$ at a generic size and fracture energy $\mathcal{G}_{\mathcal{F}}^{\infty}$ for structural size tending to infinity as:

$$\mathcal{G}_{\mathcal{F}}(d_{\max}) = \mathcal{G}_{\mathcal{F}}^{\infty}\sqrt{\frac{d_{\max}}{\phi_{\max}}}. \tag{17}$$

From Eq. (17) it is clear that the fracture energy $\mathcal{G}_\mathcal{F}$ is a statistical variable as well as $d_{\max}$ (and σ_u). Thus, to evaluate the average fracture energy as a function of the particle number N, we follow a procedure similar to the one previously described for the ultimate tensile strength. The PDF of $\mathcal{G}_\mathcal{F}$ depends on the PDF of $d_{\max}$ according to the following relationship:

$$f_{\mathcal{G}_\mathcal{F}}(\mathcal{G}_\mathcal{F}) = f_{d_{\max}}(d)\left|\frac{\mathrm{d}\, d_{\max}}{\mathrm{d}\, \mathcal{G}_\mathcal{F}}\right|. \tag{18}$$

By definition, the mean value is provided by:

$$\overline{\mathcal{G}_\mathcal{F}} = \int_{\mathcal{G}_\mathcal{F}^\infty/\sqrt{\alpha}}^{\mathcal{G}_\mathcal{F}^\infty} \mathcal{G}_\mathcal{F} f_{\mathcal{G}_\mathcal{F}}(\mathcal{G}_\mathcal{F})\, \mathrm{d}\mathcal{G}_\mathcal{F}. \tag{19}$$

Through the variable change provided by Eq. (17) and integrating by parts, the following expression for the average fracture energy can be derived as a function of the number N of grains:

$$\frac{\overline{\mathcal{G}_\mathcal{F}}}{\mathcal{G}_\mathcal{F}^\infty} = 1 - \frac{1}{5\sqrt{\alpha}(1-\beta)^N} B_{(\beta,1)}\left(-\frac{1}{5}, N+1\right). \tag{20}$$

As stated for the ultimate tensile strength, also for the fracture energy only the ratio α between maximum and minimum aggregate size plays a role, whilst the value of the maximum diameter does not affect the function shape. Results are summarized in the log–log plot of Fig. 4a, where the mean fracture energy is plotted vs. N for different α values. All the curves exhibit a similar behaviour, with two distinct ranges. In the lowest one the curves increase with a constant slope, approximately equal to 0.2, thus following a power law, whilst for larger values of N they present an asymptotic trend towards the unity. Physically speaking, this means that, increasing the number of particles considered, the probability of finding among them one with the maximum size approaches the unity, i.e. certainty. From a mechanical point of view, this yields an average fracture energy approaching $\mathcal{G}_\mathcal{F}^\infty$ for sufficiently high N values.

To highlight the scale effect upon fracture energy, we need once more the link between N and the structural size b. It could be objected that the relation between the grain number and the structural size differs from the one used for the tensile strength, since the largest grain must be sought on the fracture

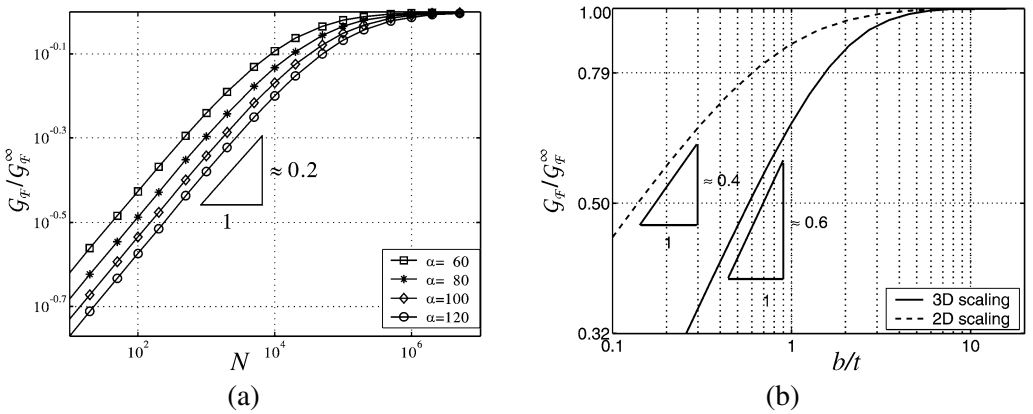

Fig. 4. Fracture energy as a function of the number of grains N surrounded by an interfacial crack (a) and size effect (b).

surface and not inside a given volume V. Nevertheless, the fact that fracture starts from the grain with the largest diameter allows us to assert that the largest grain inside V belongs to the fracture surface. The relation between the grain number and the structural size is therefore the same one used for the computation of the tensile strength of the specimen.

According to the scaling kind, different exponents characterize the small scale behaviour; on the other hand, the behaviour at large scales is independent of the considered scaling type. The small-scale scaling are respectively the following:

(a) Two-dimensional scaling: $\mathcal{G}_\mathcal{F} \approx b^{+0.4}$,
(b) Three-dimensional scaling: $\mathcal{G}_\mathcal{F} \approx b^{+0.6}$.

These two types of asymptotic behaviour are summarized in the bilogarithmic plot of Fig. 4b. Again, as can be easily argued, the higher is the order of scaling, the stronger is the size-scale effect.

5. Increase in the statistical dispersion at the smaller scales

The first moments of the PDFs of the tensile strength and of the fracture energy provide the mean values of these quantities. As shown in the previous sections, interesting considerations about their size effect can be drawn. On the other hand, also the higher order moments of the PDFs provide useful information. The second moments represent the variances of the PDFs. They contain information about the scattering of the tensile strength and fracture energy for different N values, i.e. varying the structural size. By the definition of variance:

$$\mathrm{var}[\sigma_u] = \int_{f_t}^{f_t\sqrt{\alpha}} (\sigma_u - \overline{\sigma_u})^2 f_{\sigma_u}(\sigma_u)\,\mathrm{d}\sigma_u, \tag{21}$$

$$\mathrm{var}[\mathcal{G}_\mathcal{F}] = \int_{\mathcal{G}_\mathcal{F}^\infty/\sqrt{\alpha}}^{\mathcal{G}_\mathcal{F}^\infty} (\mathcal{G}_\mathcal{F} - \overline{\mathcal{G}_\mathcal{F}})^2 f_{\mathcal{G}_\mathcal{F}}(\mathcal{G}_\mathcal{F})\,\mathrm{d}\mathcal{G}_\mathcal{F}. \tag{22}$$

The integrals in Eqs (21)–(22) can be divided into three terms. The results of two of them are straightforward, whereas the third ones can be managed integrating by parts. Therefore, in non-dimensional form, we get:

$$\frac{\mathrm{var}[\sigma_u]}{f_t^2} = \alpha - \left(\frac{\overline{\sigma_u}}{f_t}\right)^2 - \frac{2}{f_t^2}\int_{f_t}^{f_t\sqrt{\alpha}} \sigma_u F_{\sigma_u}(\sigma_u)\,\mathrm{d}\sigma_u, \tag{23}$$

$$\frac{\mathrm{var}[\mathcal{G}_\mathcal{F}]}{(\mathcal{G}_\mathcal{F}^\infty)^2} = 1 - \left(\frac{\overline{\mathcal{G}_\mathcal{F}}}{\mathcal{G}_\mathcal{F}^\infty}\right)^2 - \frac{2}{(\mathcal{G}_\mathcal{F}^\infty)^2}\int_{\mathcal{G}_\mathcal{F}^\infty/\sqrt{\alpha}}^{\mathcal{G}_\mathcal{F}^\infty} \mathcal{G}_\mathcal{F} F_{\mathcal{G}_\mathcal{F}}(\mathcal{G}_\mathcal{F})\,\mathrm{d}\mathcal{G}_\mathcal{F}. \tag{24}$$

In order to proceed, we need the cumulative distributions for the tensile strength and the fracture energy. The cumulative distribution of the largest diameter is given by Eq. (6). Since the derivative of the tensile strength with respect to the largest diameter is negative (see Eq. (9)), its cumulative distribution is given by the complement to one of the cumulative distribution of the largest diameter. On the other hand, the derivative of the fracture energy with respect to the largest diameter being positive (see Eq. (17)), its

cumulative distribution coincides with that of the largest diameter. Provided that d is substituted by σ_u and $\mathcal{G}_\mathcal{F}$ according respectively to the inverse of Eqs (9) and (17), we get:

$$F_{\sigma_u}(\sigma_u) = 1 - \left[\frac{1-\beta(\sigma_u/f_t)^5}{1-\beta}\right]^N, \tag{25}$$

$$F_{\mathcal{G}_\mathcal{F}}(\mathcal{G}_\mathcal{F}) = \left[\frac{1-\beta(G_\mathcal{F}^\infty/G_\mathcal{F})^5}{1-\beta}\right]^N. \tag{26}$$

Substituting now Eqs (25) and (26) into Eqs (23) and (24) and performing a suitable change of variables, the following expressions of the variances are finally obtained:

$$\frac{\text{var}[\sigma_u]}{f_t^2} = 1 - \left(\frac{\overline{\sigma_u}}{f_t}\right)^2 + \frac{2\alpha}{5(1-\beta)^N} B_{(\beta,1)}\left(\frac{2}{5}, N+1\right), \tag{27}$$

$$\frac{\text{var}[\mathcal{G}_\mathcal{F}]}{(\mathcal{G}_\mathcal{F}^\infty)^2} = 1 - \left(\frac{\overline{\mathcal{G}_\mathcal{F}}}{\mathcal{G}_\mathcal{F}^\infty}\right)^2 - \frac{2}{5\alpha(1-\beta)^N} B_{(\beta,1)}\left(-\frac{2}{5}, N+1\right), \tag{28}$$

where the second terms at the right hand side are provided by Eqs (12) and (20).

The non-dimensional variances are plotted in Figs 5a and 5b vs. the grain number for different values of the ratio. As can be seen, the variances increase diminishing the number of grains, i.e. as the structural size decreases; an increase of the dispersion was already predicted by Corpinteri et al. [3] for the tensile strength. The present model predicts not only a variation of the tensile strength and fracture energy values when testing specimens of different sizes, but also a wider scatter of the measured data for small sizes. Both these trends are confirmed by several experimental results (see, for instance, [10]). Furthermore, note that, in the bi-logarithmic plots of Figs 5a and 5b, the slope of the curves for large N values is the same.

Eventually, it is interesting to observe that also the third moments of the PDFs contain some useful information. The third moment represents the so-called skewness: it measures the asymmetry of a distribution. Nevertheless, for the sake of simplicity, we prefer not to compute the third moment and to highlight the effect of the asymmetry in a different way. When plotting tensile strength or fracture energy versus N, we can calculate two values, marked by subscripts 1 and 2 such that a given percentage

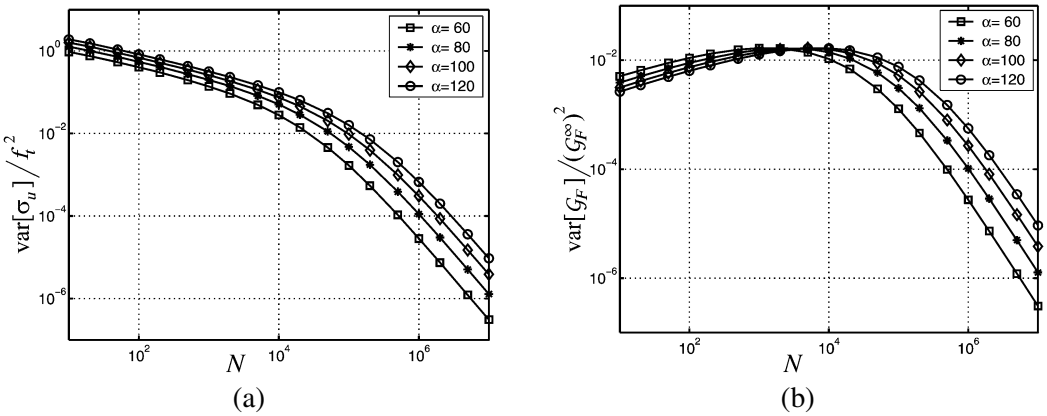

Fig. 5. Non-dimensional variance of the tensile strength (a) and of the fracture energy (b).

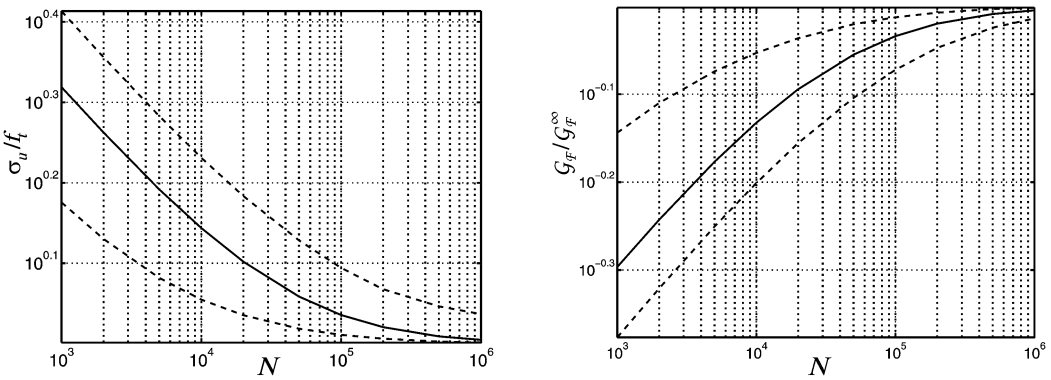

Fig. 6. Dispersion bands within 33% probability for tensile strength (a) and fracture energy (b).

$2\Delta F$ of the measured values is comprised inside this range centred on the average value. In other words, we want to compute the values corresponding to the cumulative values F_1 and F_2 defined as:

$$F_{1,2} = F(\bar{x}) \pm \Delta F, \tag{29}$$

where $\bar{x}$ can be $\overline{\sigma_u}$ or $\overline{\mathcal{G}_\mathcal{F}}$. Equations (25) and (26) provide the following values:

$$(\sigma_u)_{1,2} = f_t\sqrt{\alpha}\big[1-(1-\beta)(1-F_{1,2})^{1/N}\big]^{1/5}, \tag{30}$$

$$(\mathcal{G}_\mathcal{F})_{1,2} = \frac{\mathcal{G}_\mathcal{F}^\infty}{\sqrt{\alpha}}\big[1-(1-\beta)(F_{1,2})^{1/N}\big]^{-1/5}, \tag{31}$$

which are plotted versus N together with the average values in Figs 6a and 6b, for ΔF equal to 33%. It is evident that the mean values are not at the centre of the band. It would be if the PDFs were symmetric, but this is not the case.

At small N(small sizes), the mean strength is closer to the upper value $(\sigma_u)_1$, whereas the mean fracture energy is closer to the lower value $(\mathcal{G}_\mathcal{F})_2$. On the other hand, for large N (large sizes), the mean strength is closer to the lower value $(\sigma_u)_2$, whereas the mean fracture energy is closer to the upper value $(\mathcal{G}_\mathcal{F})_1$. For what concerns the tensile strength this means that, at small scales, the strength values are usually high but can have a sudden drop in the case a large particle (i.e. a large flaw) falls inside the higher stressed zone. On the other hand, at large scales, the strength values are usually low but can have a sudden increase in the case no large particle (i.e. no large flaw) falls inside the higher stressed zone. The opposite trends are shown by the fracture energy.

6. Variable grading

In the above treatment, the exponent of the PDF in Eq. (2) has been taken equal to 3.5. As previously remarked, this value corresponds to a concrete prepared according to the classical Füller sieve curve. Concerning concrete technology, other grading curves can be used; in particular, the so-called equal volume mix, which corresponds to an exponent equal to 4. More generally, the exponent could vary

over a not so broad range, which is comprised approximately between 3 and 4.5. Therefore, the above treatment could be re-proposed by introducing a variable exponent $2 < \tau < 3.5$ in Eq. (2), as follows:

$$f_d(d) = \frac{\tau}{1-\alpha^{-\tau}} \frac{\phi_{\min}^{\tau}}{d^{\tau+1}}. \tag{32}$$

Values of τ outside the given range are not of practical interest, since they provide a very poor packing. In fact Mayadunne et al. [11] demonstrated that the values of τ corresponding to the optimal packing are located close to 2.5. Introducing Eq. (32) into Eq. (7) and by considering the variable change given by Eq. (9), the PDF of the tensile strength is readily obtained as:

$$f_{\sigma_u}(\sigma_u) = N \frac{[1-(\sigma_u/f_t\sqrt{\alpha})^{2\tau}]^{N-1}}{(1-\alpha^{-\tau})^{N-1}} \left(\frac{2\tau}{f_t^{2\tau}\alpha^{\tau}}\right) \sigma_u^{2\tau-1}. \tag{33}$$

Computing the mean value, we obtain the average tensile strength as a function of the number N of grains. In nondimensional form:

$$\frac{\overline{\sigma_u}}{f_t} = 1 + \frac{\sqrt{\alpha}}{2\tau(1-\beta)^N} B_{(\beta,1)}\left(\frac{1}{2\tau}, N+1\right), \tag{34}$$

where now $\beta = \alpha^{-\tau}$. As can be seen, this relation generalizes Eq. (12). If we plot again, as done in Fig. 3a, the nondimensional tensile strength vs. the nondimensional structural size, the log–log plot evidences two distinct ranges. In the lowest one the curves decrease with a constant slope, whilst at the larger scales an asymptotic trend towards the unity takes over. From a mechanical point of view, this yields an average tensile strength approaching f_t for sufficiently large sizes. With respect to the previous case ($\tau = 2.5$), the slope of the slant asymptote changes: it depends on the value of τ. Results are summarized in Fig. 7, where the slope d_σ of this asymptote is plotted as a function of the exponent τ in the case of a two-dimensional scaling. As can be seen from the graph, the slope does not change strongly; however, by increasing τ (i.e. by considering less dispersed distributions), the slope of the asymptote slightly decreases. In other words, the size-scale effect is weaker. Turning the attention to concrete technology, the predicted size-scale effect on the tensile strength in the case of the equal volume grading ($\tau = 3$) is weaker than that in the case of the Füller grading.

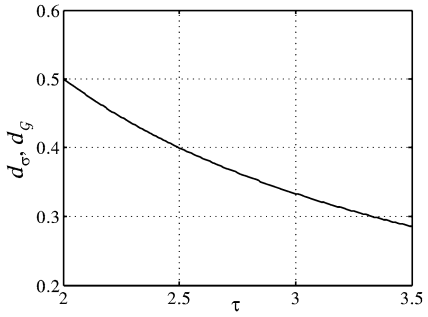

Fig. 7. Effect of the exponent τ on the slope of the slant asymptote for tensile strength (d_σ) and for fracture energy ($d_\mathcal{G}$), in the case of two-dimensional scaling.

The same procedure could be followed for the fracture toughness. By computing the PDF of $\mathcal{G}_\mathcal{F}$ starting from Eqs (17) and (7), with $f_d(d)$ given by Eq. (32) instead of Eq. (2), the following expression is obtained:

$$f_{\mathcal{G}_\mathcal{F}}(\mathcal{G}_\mathcal{F}) = N\frac{[1-(\mathcal{G}_\mathcal{F}^\infty/\mathcal{G}_\mathcal{F}\sqrt{\alpha})^{2\tau}]^{N-1}}{(1-\alpha^{-\tau})^{N-1}}2\tau(\mathcal{G}_\mathcal{F}^\infty)^{2\tau}\mathcal{G}_\mathcal{F}^{-2\tau-1}. \tag{35}$$

By computing the mean value, the average fracture toughness is obtained as a function of the number N of grains. In nondimensional form, its expression is given by:

$$\frac{\overline{\mathcal{G}_\mathcal{F}}}{\mathcal{G}_\mathcal{F}^\infty} = 1 - \frac{1}{2\tau\sqrt{\alpha}(1-\beta)^N}B_{(\beta,1)}\left(-\frac{1}{2\tau}, N+1\right). \tag{36}$$

This relation is a generalization of Eq. (20); as stated for the ultimate tensile strength, the results are similar to those represented in Fig. 3b, where the mean fracture energy is plotted vs. structural size for two- and three-dimensional scaling. Also in this case, the shape of the scaling law does not change and presents the same asymptotes; the only difference is the slope $d_\mathcal{G}$ of the slant asymptote, which is a function of the exponent τ. Its dependence on τ is very close to the one shown by d_σ, so that it can be well represented by the same curve of Fig. 7, in the case of a two-dimensional scaling. As a consequence, the same trend is predicted: if τ increases the size-scale effect results to be weaker.

7. Conclusions

In this paper, we presented a statistical approach to the size scale effects on strength and toughness of grained materials. A first important result of the present analysis is the size effect predicted, which is very close to the one provided by the Multi-Fractal Scaling Laws (MFSLs) proposed by Carpinteri and co-workers [1,2,7]:

$$\sigma_u = f_t\left[1+\frac{l_{\text{ch}}}{b}\right]^{1/2}, \tag{37}$$

$$\mathcal{G}_\mathcal{F} = \mathcal{G}_\mathcal{F}^\infty\left[1+\frac{l_{\text{ch}}}{b}\right]^{-1/2}, \tag{38}$$

respectively for tensile strength and fracture energy. l_{ch} is a length characteristic of the material, whereas b is a length proportional to the structural size. The remaining symbols have the same meaning used in the present approach.

In the Authors' opinion, the present statistical analysis confirms by another way the soundness of the fractal approach to size effect in quasi-brittle materials. There is no competition among the two approaches, since the goal of both is the same, i.e. to take into account the heterogeneity of the microstructure of the material.

More in detail, it is interesting to point out that both scaling laws present a flat asymptote for large sizes (given respectively by f_t and $\mathcal{G}_\mathcal{F}^\infty$) and a slope for small sizes equal, in absolute value, to 0.5 for the MFSLs and to 0.4 and 0.6 for the statistical analysis (2D and 3D scaling, respectively, Füller grading). In other words, we can affirm that, according to the statistical analysis, the scaling described

by the MFSLs reproduces satisfactorily the size effects of concrete structures for which scaling is two- or three-dimensional.

Furthermore, observe that the transition length (i.e. the structural dimension at which the size effect disappears), which is represented by l_{ch} in the MFSLs, is a function of the maximum aggregate diameter according to the present model. In fact, ϕ_{min} being fixed, the knee of the size effect curves shifts toward higher structural dimensions as the maximum grain size ϕ_{max} increases (see Figs 2a and 4a).

No experimental comparisons are produced within this paper, since the fit is as good as the one provided by the MFSLs. The interested reader is referred to the large amount of data analysed in the papers by Carpinteri and co-workers [12–14].

Another remarkable aspect is that the present statistical approach, even if of Weibull's type, can provide a much more complex scaling than a simple power-law, thus resulting in the presence of an intrinsic length of the material. This is more than reasonable, due to the presence of grains inside the material, and it overcomes the lack of a characteristic material length in the previous statistical theories on the ultimate strength.

Eventually, it is worth highlighting that the present approach justifies the increase of the statistical dispersion at the smaller scales for strength and toughness. This trend agrees with results from experimental investigations. Therefore, the larger scatter when testing small specimens should be carefully considered, especially if the final goal is to extrapolate strength and fracture energy values to full-size structures.

Acknowledgements

Support by the European Community is gratefully acknowledged by the authors. Thanks are also due to the Italian Ministry of Education, University and Scientific Research (MIUR).

References

[1] A. Carpinteri, Fractal nature of material microstructure and size effects on apparent mechanical properties, *Mechanics of Materials* **18** (1994), 89–101.
[2] A. Carpinteri, Scaling laws and renormalization groups for strength and toughness of disordered materials, *International Journal of Solids and Structures* **31** (1994), 291–302.
[3] A. Carpinteri, G. Ferro and S. Invernizzi, The nominal tensile strength of disordered materials: a statistical fracture mechanics approach, *Engineering Fracture Mechanics* **58** (1997), 421–435.
[4] A. Carpinteri, P. Cornetti and S. Puzzi, A stereological analysis of aggregate grading and size effect on concrete tensile strength, *International Journal of Fracture* **128** (2004), 233–242.
[5] P. Stroeven, A stereological approach to roughness of fracture surfaces and tortuosity of transport paths in concrete, *Cement and Concrete Composites* **22** (2000), 331–341.
[6] A. Carpinteri and P. Cornetti, Size effects on concrete tensile fracture properties: an interpretation of the fractal approach based on the aggregate grading, *Journal of the Mechanical Behaviour of Materials* **13** (2002), 233–246.
[7] A. Carpinteri, B. Chiaia and P. Cornetti, A scale-invariant cohesive crack model for quasi-brittle materials, *Engineering Fracture Mechanics* **69** (2002), 207–217.
[8] S. Wolinski, D.A. Hordijk, H.W. Reinhardt and H.A.W. Cornelissen, Influence of aggregate size on fracture mechanics of parameters of concrete, *International Journal of Cement Composites and Lightweight Concrete* **9** (1987), 95–103.
[9] Q. Li, Y. Duan and G. Wang, Behaviour of large concrete specimens in uniaxial tension, *Magazine of Concrete Research* **54** (2002), 385–391.
[10] B.L. Karihaloo, H.M. Abdalla and Q.Z. Xiao, Size effect in concrete beams, *Engineering Fracture Mechanics* **70** (2003), 979–993.
[11] A. Mayadunne, S.N. Bhattacharia and E. Kosior, Modelling of packing behaviour of irregularly shaped particles dispersed in a polymer matrix, *Powder Technology* **89** (1996), 115–127.

[12] A. Carpinteri, B. Chiaia and G. Ferro, Size effects on nominal tensile strength of concrete structures: multifractality of material ligaments and dimensional transition from order to disorder, *Materials & Structures* **28** (1995), 311–317.
[13] A. Carpinteri and B. Chiaia, Multifractal nature of concrete fracture surfaces and size effects on nominal fracture energy, *Materials & Structures* **28** (1995), 435–443.
[14] A. Carpinteri, B. Chiaia and G. Ferro, Multifractal scaling law: an extensive application to nominal strength size effect of concrete structures, *Atti del Dipartimento di Ingegneria Strutturale*, Politecnico di Torino, No. 51 (1995).